2018

# Influence of system bandwidth on self-mixing signal

Bin Liu
*University of Wollongong*, bl987@uowmail.edu.au

Yuxi Ruan
*University of Wollongong*, yr776@uowmail.edu.au

Lingzhi Cao
*Zhengzhou University of Light Industry*

Yanguang Yu
*University of Wollongong*, yanguang@uow.edu.au

Jiangtao Xi
*University of Wollongong*, jiangtao@uow.edu.au

*See next page for additional authors*

# Influence of system bandwidth on self-mixing signal


## Abstract

Self-mixing interferometry (SMI) is a well-developed sensing technology. An SMI system can be described using a model derived from the well-known Lang and Kobayashi equations by setting the system operating in stable region. The features of an SMI signal are determined by the external optical feedback factor (denoted by C). Our recent work shows that when the factor C increases to a certain value, e.g. in moderate feedback regime with 1





## Publication Details

B. Liu, Y. Ruan, L. Cao, Y. Yu, J. Xi, Q. Guo & J. Tong, "Influence of system bandwidth on self-mixing signal," in Semiconductor Lasers and Applications VIII, 2018, pp. 1081210-1-1081210-6.



## Authors

Bin Liu, Yuxi Ruan, Lingzhi Cao, Yanguang Yu, Jiangtao Xi, Qinghua Guo, and Jun Tong

# Influence of system bandwidth on self-mixing signal

Bin Liu, Yuxi Ruan, Lingzhi Cao, Yanguang Yu, Jiangtao Xi, et al.

Bin Liu, Yuxi Ruan, Lingzhi Cao, Yanguang Yu, Jiangtao Xi, Qinghua Guo, Jun Tong, "Influence of system bandwidth on self-mixing signal," Proc. SPIE 10812, Semiconductor Lasers and Applications VIII, 1081210 (6 November 2018); doi: 10.1117/12.2500737

SPIE.

Event: SPIE/COS Photonics Asia, 2018, Beijing, China

# Influence of System Bandwidth on Self-mixing Signal

Bin Liu[a], Yuxi Ruan[a], Lingzhi Cao[*b], Yanguang Yu[a], Jiangtao Xi[a], Qinghua Guo[a], and Jun Tong[a]
[a]School of Electrical, Computer and Telecommunications Engineering, University of Wollongong, Wollongong, NSW, 2522, Australia; [b]School of Electrical and Information Engineering, Zhengzhou University of Light Industry, Zhengzhou, Henan, 450000, China

## ABSTRACT

Self-mixing interferometry (SMI) is a well-developed sensing technology. An SMI system can be described using a model derived from the well-known Lang and Kobayashi equations by setting the system operating in stable region. The features of an SMI signal are determined by the external optical feedback factor (denoted by *C*). Our recent work shows that when the factor *C* increases to a certain value, e.g. in moderate feedback regime with 1<C<4.6, the SMI system might enter unstable region and the existing SMI model is invalid. In this case, the SMI signals exhibit some novel features and contain higher-frequency components. To detect an SMI signal without distortion or take suitable correction on the SMI signal, it is must to make an analysis on the system bandwidth and its influence on SMI signals. The results in this paper provide useful guidance for developing an SMI sensing system.

**Keywords:** self-mixing interferometry, laser diode, optical feedback, frequency bandwidth

## 1. INTRODUCTION

As a promising non-contact sensing technology, self-mixing interferometry (SMI) has attracted much attention of researchers in recent decades. The SMI is based on the self-mixing effect that occurs when a fraction of light back-reflected or back-scattered by an external target reenters the laser inside cavity [1-4]. In this case, both the laser output power and frequency is modulated. The modulated laser output is usually considered as the SMI signal. A typical self-mixing laser diode (SMLD) sensor consists of laser diode (LD), a photodiode (PD) packaged in the rear of the LD, a lens and external target, as shown in Figure 1. As a minimum part-count scheme, various SMI-based applications have been developed in the industrial and laboratory environment, such as measurement of displacement, velocity, vibration, alpha factor, refraction index, strain, acoustic emission, etc.[5-10].

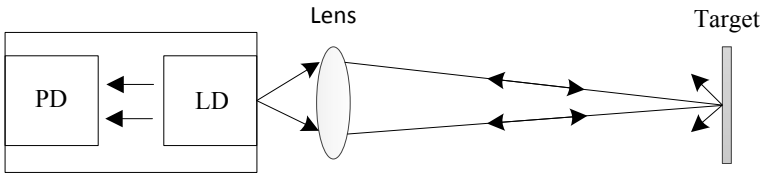


Figure 1. Basic structure of an SMLD system

Most of the SMLD-based applications are based on the stable SMI mathematic model shown in Equation (1) and (2),

$$\phi_F(t) = \phi_0(t) - C\sin(\phi_F(t) + \arctan\alpha) \tag{1}$$

$$P(t) = P_0(1 + m \times \cos(\phi_F(t)) \tag{2}$$

where $\phi_F(t)$ and $\phi_0(t)$ are the external light phases at the location of the target for the LD with and without feedback respectively, $P(t)$ and $P_0$ is the power emitted by the LD with and without optical feedback respectively, $m$ is the

Semiconductor Lasers and Applications VIII, edited by Ning Hua Zhu, Werner H. Hofmann, Proc. of SPIE
Vol. 10812, 1081210 · © 2018 SPIE · CCC code: 0277-786X/18/$18 · doi: 10.1117/12.2500737

modulation index (with typical values ~$10^{-3}$), C is the optical feedback level factor and $\alpha$ is the linewidth enhancement factor. The modulated laser power $P(t)$ is the SMI signal. which is derived from the steady-state solution of the Lang and Kobayashi (L-K) equations [11], or from the classical three-mirror model [5], by assuming the SMLD system operates in stable mode, i.e. both the electric field and carrier density in an LD with a stationary external cavity can reach a constant state after a transient period.

The SMI signal can then be acquired by the detection circuit and used for extracting useful information. It is usually desired that an SMI operates in a stable mode, in which case the SMI signal contains sinusoidal-like fringes or sawtooth-like fringes. The shape of an SMI signal is characterized by a parameter called the feedback level factor which is denoted as *C* and expressed as:

$$C = \frac{\kappa}{\tau_{in}} \tau \sqrt{1+\alpha^2} \tag{3}$$

where $\kappa$ is the feedback strength and $\tau$ is the external cavity light round-trip time, $\tau_{in}$ is the internal cavity light round-trip time, $\alpha$ is the linewidth enhancement factor. Based on the value of C, the SMLD system may operate in weak feedback regime (C<1), moderate feedback regime (1<C<4.6) or strong feedback regime (C>4.6). In weak feedback regime, the SMI signals show sinusoidal-like fringes which are similar to the tradition interference fringes. In moderate or strong feedback regime, the SMI signal shows asymmetric hysteresis and produces sawtooth-like fringes [12-15]. Figure 2 shows typical SMI signals for different feedback level factors when the external target has a sinusoidal displacement. Figure 2 (a) is the target displacement, (b) (c) is the corresponding normalized SMI signal with C=0.5 and C=3.5 respectively.

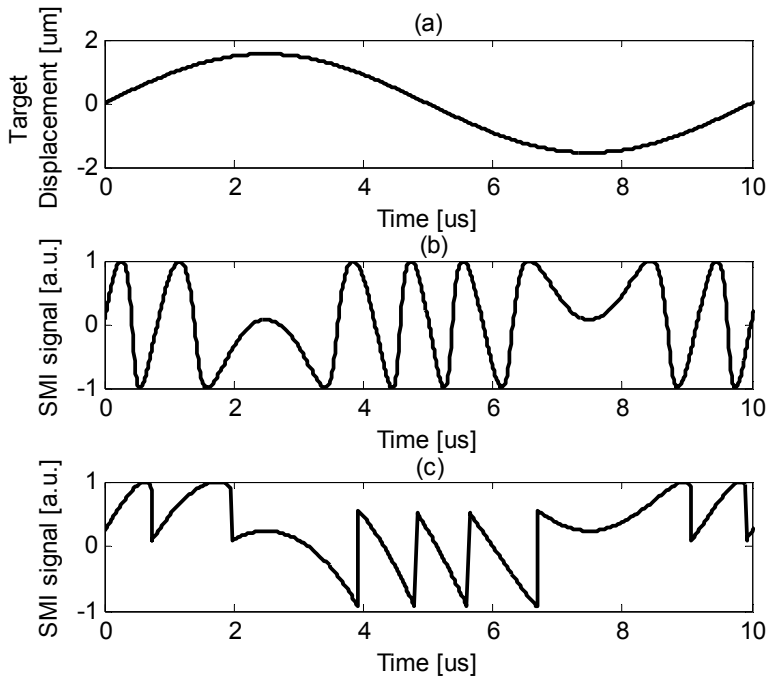


Figure 2: Stable SMI signals with different *C* values, (a) the trace of the target movement, (b) the SMI signal when *C*=0.5, (c) the SMI signal when *C*=3.5.

Most of the SMLD-based applications are based on the stable SMI mathematic model. However, when the SMLD system operates in moderate or strong feedback regime, some dynamics or new features may happen in the SMI signals which cannot be explained by using the stable SMI mathematic model. In 2012, Teysseyre et al. [16] found damped oscillation in sawtooth-like SMI signals. In this work, the external target is located more than one meter away from the LD. It was found that damped oscillation appears on the discontinuous point of the SMI signal when the SMLD system operates in moderate feedback regime and this kind of damped oscillation corresponds to the external cavity mode, which contains information on the target distance and reflectivity. Additionally, our recent work [17, 18] shows another

kind of oscillation, i.e. undamped relaxation oscillation (RO), may occur when the SMLD operates in moderate or strong feedback regime. In this case, SMI signals may exhibit some new and complicate features. These features may be not observed in the experiments although they virtually exist. Incomplete or distorted SMI signals may be captured due to the limitation of SMI system bandwidth.

In this paper, we investigate the influence of the system bandwidth on SMI signals via numerical simulations on the well-known Lang and Kobayashi equations. It shows that undamped RO and damped external cavity mode oscillation may simultaneously exist in the SMI signals when the SMLD system in moderate feedback regime. The signal detection system with different bandwidth may detect different SMI signals.

## 2. THEORY

Since the stable SMI model is not able to explain the dynamics appearing in the SMI signal when the system is in moderate or strong feedback regime, we need to start from the original L-K equations [11], which can be used to describe the dynamics of an LD with optical feedback, shown in Equation (4)-(6). There are three main variables, i.e. electric field amplitude $E(t)$, electric field phase $\phi(t)$, carrier density $N(t)$ in the equations. The laser intensity $P(t)$ is usually expressed as $P(t)=E^2(t)$, which is also considered as the SMI signal.

$$\frac{dE(t)}{dt}=\frac{1}{2}\left\{G\left[N(t),E(t)\right]-\frac{1}{\tau_p}\right\}E(t)+\frac{\kappa}{\tau_{in}}\cdot E(t-\tau)\cdot\cos\left[\omega_0\tau+\phi(t)-\phi(t-\tau)\right] \tag{4}$$

$$\frac{d\phi(t)}{dt}=\frac{1}{2}\alpha\left\{G\left[N(t),E(t)\right]-\frac{1}{\tau_p}\right\}-\frac{\kappa}{\tau_{in}}\cdot\frac{E(t-\tau)}{E(t)}\cdot\sin\left[\omega_0\tau+\phi(t)-\phi(t-\tau)\right] \tag{5}$$

$$\frac{dN(t)}{dt}=J-\frac{N(t)}{\tau_s}-G\left[N(t),E(t)\right]E^2(t) \tag{6}$$

where, $G\left[N(t),E(t)\right]=G_N\left[N(t)-N_0\right]\left[1-\varepsilon\Gamma E^2(t)\right]$ is the modal gain per unit time. The physical meanings and typical values of the other symbols appearing in (4)-(5) are shown in Table 1, which are adopted from [19, 20].

Table 1. Meanings of the symbols in the L-K equations

| Symbol | Physical Meaning | Value |
|---|---|---|
| $E(t)$ | amplitude of the intra-cavity electric field | |
| $\phi(t)$ | phase of the intra-cavity electric field, $\phi(t)=[\omega(t)-\omega_0]t$ | |
| $\omega(t)$ | laser angular frequency with feedback | |
| $\omega_0$ | laser angular frequency without feedback | $2.42\times10^{15}\ rads^{-1}$ |
| $N(t)$ | carrier density | |
| $G_N$ | modal gain coefficient | $8.1\times10^{-13}\ m^3s^{-1}$ |
| $N_0$ | carrier density at transparency | $1.1\times10^{24}\ m^{-3}$ |
| $\varepsilon$ | nonlinear gain compression coefficient | $2.5\times10^{-23}\ m^3$ |
| $\Gamma$ | confinement factor | 3 |
| $\tau_p$ | photon life time | $2.0\times10^{-12}\ s$ |
| $\kappa$ | feedback strength | |
| $\tau_{in}$ | internal cavity round-trip time | $8.0\times10^{-12}\ s$ |
| $\alpha$ | line-width enhancement factor | 6 |
| $J$ | injection current | |
| $\tau_s$ | carrier life time | $2.0\times10^{-9}\ s$ |
| $\tau$ | light roundtrip time in the external cavity, $\tau=2L/c$ | |
| $L$ | external cavity length | |

The widely accepted mathematical model for describing an SMI waveform , i.e. Eq. (1)-(2), is derived from the steady state solutions of the L-K equations by setting $dE(t)/dt = 0$ , $d\phi(t)/dt = \omega_s - \omega_0$ and $dN(t)/dt = 0$ . However, this stable model is not able to describe the details of the SMI waveforms in some cases [16-18] In order to obtain the complete SMI signal, all the simulations in this work are based on numerical simulations for L-K equations.

## 3. SIMULATION AND ANALYSIS

For SMI-based applications, the external target is usually moving. In this case, the external cavity length can be expressed as $L=L_0+\Delta L$ , where $L_0$ is the initial external cavity length, $\Delta L$ is the displacement of the target. We assume $\Delta L$ is in a sinusoidal law with a frequency of 40KHz and amplitude of $1.5\lambda_0$ , where $\lambda_0$ is the unperturbed laser wavelength. Considering a typical case for an SMI system in moderate feedback regime, i.e. C=2.5, the simulation results is depicted in Figure 3, where Figure 3(a) is the displacement of the external target, Figure 3(b) is the corresponding SMI signal, Figure 3(c) is the spectrum of the SMI signal. From Figure 3, it can be found the RO frequency in the SMI signal in Figure 3(b) is about 2.3 GHz. Meanwhile, based on [16], the corresponding frequency of the external cavity mode can be calculated as $1/(2L_0/c+\tau_{offset})$ ,where c is the light speed in vacuum, $\tau_{offset}$ is off-set which depends on the feedback strength, with typical values of several times of 0.1ns, e.g. for $\tau_{offset}$=0.5 $ns$ , the frequency of the external cavity mode is about 680 MHz .

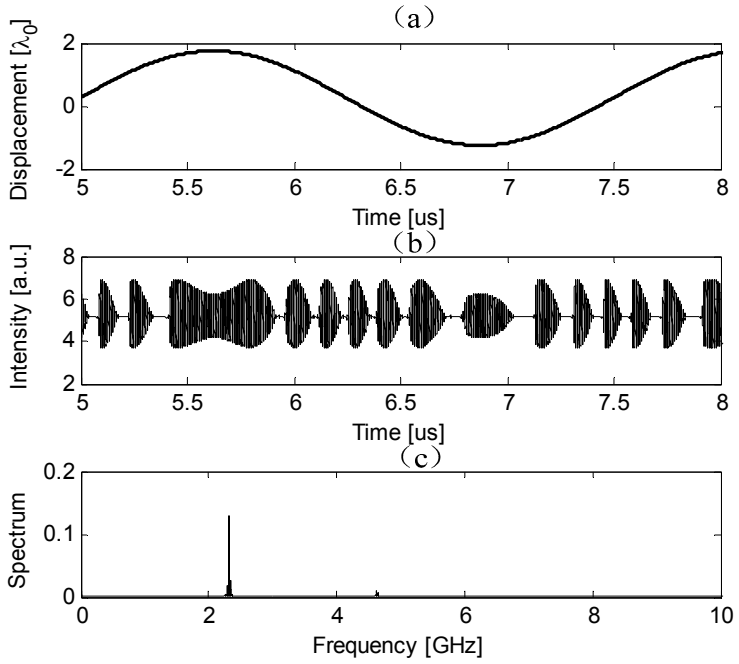


Figure 3. Simulation results for the modulated intensity scaled as $E^2(t)/10^{20}$ when $J$=1.3$J_{th}$ , $L_0$=0.16 $m$ , $\alpha = 6$ and $C = 2.5$ . (a) Displacement of target, (b) Corresponding SMI signal, (c) Spectrum of signal in (b)

The SMI signal is usually detected by the photodiode packaged at the rear of the LD together with a trans-impedance amplifier. The rising time of the packaged PD is usually several nano second, corresponding to a bandwidth of several hundred MHz. However, the bandwidth of the trans-impedance amplifier is usually from several hundred KHz to several ten MHz, e.g. the detection circuit for conventional SMI signals in work [6, 10] has a bandwidth of 10 MHz. Therefore, we apply a low-pass filter with cut-off frequency of 800 MHz and 10 MHz respectively on the SMI signal in Figure 3(b). Figure 4 shows the filtered SMI signals with different cut-off frequency, where Figure 4(a) is the original SMI signal as in Figure 3(b). Applying a low-pass filter with cut-off

frequency of 800MHz on Figure 4(a), we can obtain the filtered signal as shown in Figure 4(b). Figure 4(c) is the enlargement of the 'T area in (b)'. From (b) and (c), damped oscillation with an frequency corresponding to the external cavity mode (around 700 MHz) is clearly shown at discontinuities of the SMI signal. Additionally, the maximum peak-peak value of the external cavity mode oscillation is about 0.056 as shown in (c), whereas the maximum peak-peak value of the relaxation oscillation is about 3.179 as shown in (a), more than 50 times larger than the external cavity mode oscillation. Figure 4(d) is the filtered SMI signal with a low-pass filter with cut-off frequency of 10 MHz, it can be seen from which the relaxation oscillation and external cavity mode oscillation are filtered, showing a conventional SMI as in the literature[5-7].

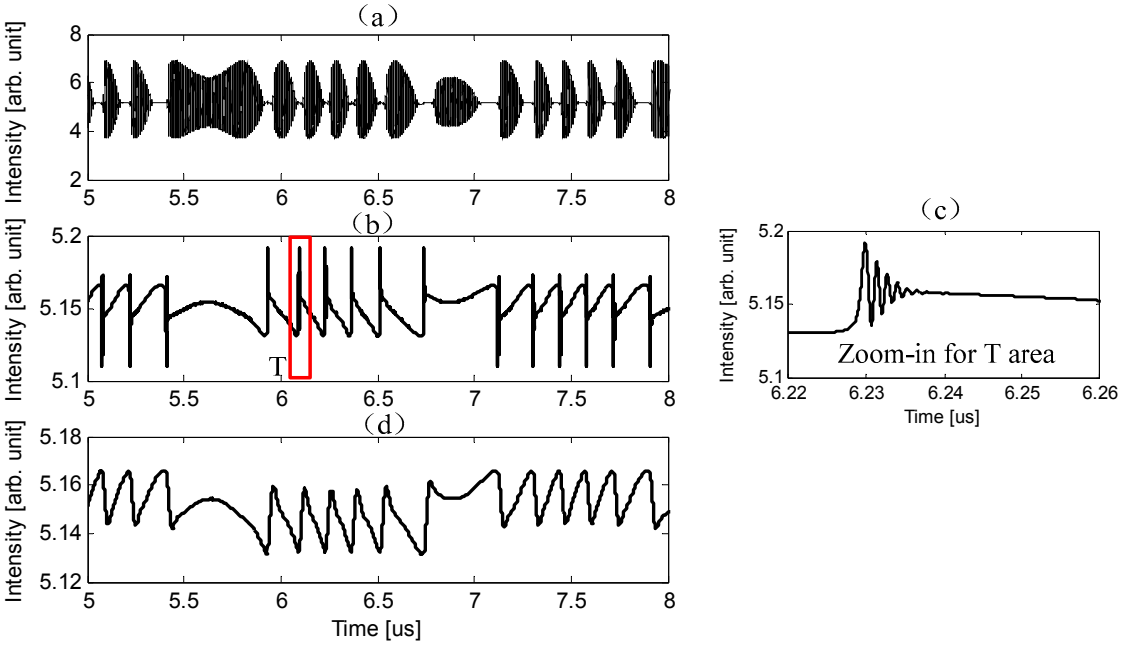


Figure 4 Filtered SMI signal with different cut-off frequency, (a) the original SMI signal, (b) filtered SMI signal with cut-off frequency of 800 MHz,, (c) the enlargement of 'T area' in (b), (d) filtered SMI signal with cut-off frequency of 10 MHz.

From above analysis, it can be concluded that there are two kinds of high-frequency oscillations in the SMI signals when the SMLD in moderate feedback regime with undamped RO. One is the relaxation oscillation and the other is the external cavity mode oscillation. Furtherly, the magnitude of the relaxation oscillation is much stronger than the external cavity mode oscillation. By applying a low-pass filter with proper cut-off frequency, the SMI signal containing damped external cavity mode oscillation as in [16] can be got. Finally, the conventional SMI signals can be obtained by applying a low-pass filter with cut-off frequency lower than the relaxation oscillation and external cavity mode oscillation frequency on the SMI signals.

## 4. CONCLUSION

The influence of the system bandwidth on SMI signals is investigated. It is analyzed via numerical simulations on the well-known Lang and Kobayashi equations, which shows that undamped RO and damped external cavity mode oscillation may exist in the SMI signals when the SMLD system is in moderate feedback regime. Additionally, the relaxation oscillation is much stronger than the external cavity mode oscillation. The signal detection system with different bandwidth detects different SMI signals. It is demonstrated that the bandwidth of the photodetector is of great significance for detecting the completed and true SMI signal. The results in this paper provide useful guidance for developing an SMLD sensing system.

## REFERENCES


[1] S. Donati, G. Giuliani, and S. Merlo, "Laser diode feedback interferometer for measurement of displacements without ambiguity," IEEE journal of quantum electronics, **31**(1), 113-119,(1995).

[2] S. Donati, "Developing self-mixing interferometry for instrumentation and measurements," Laser & Photonics Reviews, **6**(3), 393-417,(2012).

[3] Y. Yu, G. Giuliani, and S. Donati, "Measurement of the linewidth enhancement factor of semiconductor lasers based on the optical feedback self-mixing effect," Photonics Technology Letters, IEEE, **16**(4), 990-992,(2004).

[4] Y. Yu, J. Xi, J. F. Chicharo, and T. M. Bosch, "Optical Feedback Self-Mixing Interferometry With a Large Feedback Factor C: Behavior Studies," Quantum Electronics, IEEE Journal of, **45**(7), 840-848,(2009).

[5] T. Taimre, M. Nikolić, K. Bertling, Y. L. Lim, T. Bosch, and A. D. Rakić, "Laser feedback interferometry: a tutorial on the self-mixing effect for coherent sensing," Advances in Optics and Photonics, **7**(3), 570-631,(2015).

[6] B. Liu, Y. Ruan, Y. Yu, J. Xi, Q. Guo *et al.*, "Laser self-mixing fiber Bragg grating sensor for acoustic emission measurement," Sensors, **18**(6), 1956,(2018).

[7] D. Guo, L. Shi, Y. Yu, W. Xia, and M. Wang, "Micro-displacement reconstruction using a laser self-mixing grating interferometer with multiple-diffraction," Optics express, **25**(25), 31394-31406,(2017).

[8] Y. Yu, J. Xi, J. F. Chicharo, and T. Bosch, "Toward automatic measurement of the linewidth-enhancement factor using optical feedback self-mixing interferometry with weak optical feedback," Quantum Electronics, IEEE Journal of, **43**(7), 527-534,(2007).

[9] Y. Yu, J. Xi, and J. F. Chicharo, "Measuring the feedback parameter of a semiconductor laser with external optical feedback," Optics express, **19**(10), 9582-9593,(2011).

[10] K. Lin, Y. Yu, J. Xi, H. Li, Q. Guo *et al.*, "A Fiber-Coupled Self-Mixing Laser Diode for the Measurement of Young's Modulus," Sensors, **16**(6), 928,(2016).

[11] R. Lang and K. Kobayashi, "External optical feedback effects on semiconductor injection laser properties," Quantum Electronics, IEEE Journal of, **16**(3), 347-355,(1980).

[12] G. Giuliani, M. Norgia, S. Donati, and T. Bosch, "Laser diode self-mixing technique for sensing applications," Journal of Optics A: Pure and Applied Optics, **4**(6), S283,(2002).

[13] T. Bosch and S. Donati, "Optical feedback interferometry for sensing application," Optical engineering, **40**(1), 20-27,(2001).

[14] J. Xi, Y. Yu, J. F. Chicharo, and T. Bosch, "Estimating the parameters of semiconductor lasers based on weak optical feedback self-mixing interferometry," Quantum Electronics, IEEE Journal of, **41**(8), 1058-1064,(2005).

[15] U. Zabit, F. Bony, T. Bosch, and A. D. Rakic, "A self-mixing displacement sensor with fringe-loss compensation for harmonic vibrations," IEEE Photonics Technology Letters, **22**(6), 410-412,(2010).

[16] R. Teysseyre, F. Bony, J. Perchoux, and T. Bosch, "Laser dynamics in sawtooth-like self-mixing signals," Optics letters, **37**(18), 3771-3773,(2012).

[17] Y. Fan, Y. Yu, J. Xi, and Q. Guo, "Dynamic stability analysis for a self-mixing interferometry system," Optics express, **22**(23), 29260-29269,(2014).

[18] B. Liu, Y. Yu, J. Xi, Y. Fan, Q. Guo *et al.*, "Features of a self-mixing laser diode operating near relaxation oscillation," Sensors, **16**(9), 1546,(2016).

[19] B. Tromborg, J. H. Osmundsen, and H. Olesen, "Stability analysis for a semiconductor laser in an external cavity," Quantum Electronics, IEEE Journal of, **20**(9), 1023-1032,(1984).

[20] B. Liu, Y. Yu, J. Xi, Q. Guo, J. Tong, and R. A. Lewis, "Displacement sensing using the relaxation oscillation frequency of a laser diode with optical feedback," Applied optics, **56**(24), 6962-6966,(2017).